Radiation Protection Dosimetry (2004), Vol. 109, No. 3, pp. 225–234
DOI: 10.1093/rpd/nch046

SIMULATION OF THE EXPERIMENTAL PRE-DOSE TECHNIQUE FOR RETROSPECTIVE DOSIMETRY IN QUARTZ

Vasilis Pagonis* and Hezekiah Carty
Physics Department, McDaniel College, Westminster, MD 21158, USA

Received November 3 2003, amended March 12 2004, accepted March 16 2004

The pre-dose technique of thermoluminescence for quartz has been used extensively for retrospective dosimetry of quartz and other natural materials. A recently published model that is a modification of the well-known Zimmerman theory is used here to simulate the complete sequence of experimental steps taken during the additive dose version of the pre-dose technique. The results of simulation show how the method can reproduce accurately the accumulated dose or paleodose received by the sample. The solution of the kinetic differential equations elucidates the various electron and hole processes taking place during the experimental pre-dose procedure and shows clearly the mechanism of hole transfer from the reservoir to the luminescence centre caused by heating to the activation temperature. The numerical results show that the pre-dose technique can reproduce the paleodose with an accuracy of ±1–5%, even when the paleodose is varied over more than an order of magnitude. New quantitative results are presented for the effect of the test dose and of the calibration beta dose, β, on the accuracy of the pre-dose technique. The conclusions drawn from the simple model for quartz can be used to make improvements to more general quartz models.

INTRODUCTION

The pre-dose technique is a well-established experimental method for determining the total cumulative dose from natural radiation sources and for accident dosimetry[1,2]. The method is based on the observed change of sensitivity of the '110°C' thermoluminescence (TL) peak of quartz, caused by a combination of irradiation and high temperature annealing[3].

During the past 20 y several researchers have shown that natural materials containing quartz can be used as environmental dosemeters. The range of doses that can be estimated using the pre-dose technique has been shown to range from low values of a few tens of milligrays to larger doses of the order of several grays. Bailiff and Haskell[4] measured the thermal characteristics of Japanese tiles and showed that the pre-dose technique can be used to measure low doses in the region of 10 mGy. Stoneham[5] applied several pre-dose techniques to artificially irradiated porcelain fragments and showed that porcelain would be a good pre-dose dosemeter for both low doses (44 mGy) and high doses (440 mGy). Haskell *et al.*[6] applied the pre-dose TL technique to measure the cumulative dose to bricks exposed to fallout radiation during atmospheric testing at the Nevada site and estimated doses as low as 0.20 Gy. Haskell *et al.*[7] measured the cumulative dose to quartz crystals embedded in housing bricks that were used for construction shortly before the fallout incidents in Utah. They obtained an average dose of 38 ± 15 mGy. Hutt *et al.*[8] used the pre-dose, fine grain and quartz inclusion TL techniques to analyse the cumulative dose to a variety of environmental materials in regions downwind from Chernobyl. These authors obtained dose estimates in the range 0.1–2 Gy.

Although the above experimental studies showed the feasibility of using quartz as an environmental dosemeter, many of the experimental protocols used in pre-dose TL dosimetry are of an empirical nature, necessitating a better theoretical understanding and modelling of the pre-dose phenomenon.

Recently, Chen and Leung[9,10] developed a mathematical model for the pre-dose effect on quartz, which is based on two electron and two hole trapping states. The model is a modification of the Zimmerman theory, which explained first the pre-dose effect[11,12]. Chen and Leung[9,10] simulated a typical sequence of experimental actions taken during the pre-dose experimental technique, consisting of a sequence of irradiations and annealings. By using physical arguments concerning the observed experimental behaviour of quartz samples, these authors were able to arrive at a 'good' set of parameters for their model and explained successfully several experimental results associated with the pre-dose effect in quartz. These experimental results are discussed further in subsequent sections.

The purpose of the present paper is to show that the model of Chen and Leung[9,10] can also be used to simulate successfully the complete sequence of experimental steps taken during the additive dose variation of the pre-dose technique. The solution of the kinetic differential equations elucidates the various electron and hole processes taking place and shows clearly that heating to the activation temperature causes a hole transfer from the reservoir (R) to the luminescence centre (L).

*Corresponding author: vpagonis@mcdaniel.edu

To the best of the authors' knowledge, the complete sequence of events in the pre-dose technique has not been simulated numerically before. Furthermore, the present simulation gives new quantitative results for the effect of several experimental parameters on the estimated accrued dose.

The numerical results show that within the limitations of the present simulation, the pre-dose technique can reproduce the paleodose (PD) with an accuracy of ±1–5% or better. The accuracy of the method remains within the ±5% limit when the PD is varied over at least an order of magnitude.

Quantitative results are also obtained for the effect of the test dose (TD) and of the calibration beta dose, β, on the accuracy of the pre-dose method in retrospective dosimetry.

THE ADDITIVE DOSE VARIATION OF THE PRE-DOSE TECHNIQUE

Two main variations of the pre-dose technique in TL exist, known as the multiple thermal activation technique and the additive dose technique. The basic sequence of measurements made during the additive dose technique is as follows[3].

Two portions (aliquots) of the sample are used. Using the first portion, the following steps are implemented in order to measure the TL sensitivities S_o and S_N of the material to a small TD:

(1) Give a TD (usually 0.01 Gy) and measure the 110°C peak response, denoted by S_o.
(2) Heat to the activation temperature of 500°C, as in the course of a normal TL glow curve.
(3) Give the same TD and measure the activated 110°C response, denoted by S_N.

Using the second portion of the material, the TL sensitivities S_o and $S_{N+\beta}$ are measured as follows:

(4) Repeat a measurement of the 110°C peak response, S_o, as in step 1 above. This is done for sample normalisation purposes between the two aliquots.
(5) Give a laboratory calibrating dose β, usually several grays.
(6) Heat again to the activation temperature of 500°C as in step 2 above.
(7) Give the same TD and measure the new response, denoted by $S_{N+\beta}$.

The response to the TD is measured by heating the sample to 150°C, just above the '110°C' TL peak. This additive dose variation of the pre-dose technique avoids the well-known complications arising from the phenomenon of radiation quenching[3]. In addition, the additive dose method avoids multiple thermal activation of the material, which can cause changes to its pre-dose characteristics.

By assuming that the change in sensitivity, $S_N - S_o$, between steps 1 and 3 above is proportional to the accrued dose during the lifetime of the material and that the further increase, $S_{N+\beta} - S_o$, between steps 4 and 7 is proportional to the calibrating dose, β, the accrued dose (AD) can be calculated using the equation[3]

$$AD = \frac{S_N - S_o}{S_{N+\beta} - S_o} \cdot \beta. \quad (1)$$

DESCRIPTION OF THE MODIFIED ZIMMERMAN PRE-DOSE MODEL

Zimmerman[11,12] first proposed a pre-dose model consisting of one electron trapping state T, a luminescence centre L and a hole reservoir R. Chen[13] proposed a modification of the Zimmerman model by adding an extra electron level, S, that competes for electrons during the heating stage. By using physical arguments concerning the observed experimental behaviour of quartz samples, Chen and Leung[9,10] showed that their modified Zimmerman model explained successfully the following experimental results:

(1) linear dependence of the TL signal on the test dose
(2) exponential approach of the sensitivity to saturation with repeated additive doses
(3) quenching by high dose exposure, UV reversal and the distinction between reservoir and centre saturations.

The energy scheme used by Chen and Leung[9,10] consists of two trapping states T and S, the luminescence centre L and the hole reservoir R, with total concentrations N_t, N_s and N_r (in cm^{-3}) and with instantaneous occupancies denoted by n_t, n_s and n_r (in cm^{-3}), correspondingly. M and m denote, respectively, the total concentration and instantaneous occupancy of the hole centres (cm^{-3}) in the luminescence centre, L. A_m and A_1 ($cm^3\ s^{-1}$) are, respectively, the recombination and trapping probability coefficients of electrons and holes in L.

The activation energy for the main traps T is E_t (in electron volts) and the frequency factor is $s_t(s^{-1})$, while the competitor traps S are considered to be thermally disconnected. The activation energy for the hole reservoir, R, is E_r (in electron volts) and the frequency factor is $s_r(s^{-1})$. The retrapping probability coefficients for R, T and S are denoted, respectively, by A_r, A_t and A_s (in $cm^3\ s^{-1}$), and n_c and n_v (cm^{-3}) represent the concentrations of electrons and holes in the conduction and valence bands, respectively. The rate of production of electron–hole pairs x (in $cm^{-3}\ s^{-1}$) is proportional to the dose rate, and the dose is proportional to $D = x \cdot t$,

Table 1. The parameters used in the model of Chen and Leung[9,10] and in this paper.

Chen and Leung[9,10]	Modified values used here
$E_t = 1.0$ eV	
$s_t = 10^{13}$ s^{-1}	
$E_r = 1.4$ eV	1.8
$s_r = 10^{13}$ s^{-1}	
$x \cdot t = 5 \times 10^{10}$ cm^{-3}	
$A_r = 10^{-10}$ cm^3 s^{-1}	
$N_r = 10^{13}$ cm^{-3}	10^{14}
$M = 10^{14}$ cm^{-3}	
$A_s = 10^{-11}$ cm^3 s^{-1}	0.5×10^{-11}
$A_m = 10^{-12}$ cm^3 s^{-1}	
$A_t = 10^{-12}$ cm^3 s^{-1}	
$N_t = 10^{13}$ cm^{-3}	
$N_s = 10^{12}$ cm^{-3}	1.01×10^{13}
$A_1 = 10^{-12}$ cm^3 s^{-1}	

The numbers in the third column show the modified values used in this paper when they are different from those of Chen and Leung[9,10].

where t is the irradiation time in seconds and D is in cm^{-3} (or more accurately, in electrons cm^{-3} or holes cm^{-3}).

The differential equations for the excitation and heating stages are given in Chen and Leung[9,10] and will not be repeated here. After each excitation stage, the simulation uses a relaxation period in which the temperature of the sample is kept constant at room temperature for 60 s after the excitation has stopped ($x = 0$), and the concentrations of n_c and n_v decay to negligible values. This value of the relaxation time is indeed found sufficient for n_c and n_v to reach negligible values. It is not possible to obtain an exact value for the relaxation decay rate from the delocalised bands since the simulation seems to indicate that this process is essentially instantaneous. The relaxation time is estimated to be much less than 1 ms, which represents the time resolution of the differential equation solver in Mathematica.

After each heating cycle to 150 or 500°C, the model simulates a cooling-down period with a constant cooling rate of $\beta = -5$°C s^{-1}.

A linear heating rate $\beta = +5$°C s^{-1} is used during the simulation of the TL glow curves, so that $T = T_o + \beta t$ and $x = 0$ during the readout stage. The emitted light is taken to be proportional to the rate of recombination, so that

$$I = -\mathrm{d}m/\mathrm{d}t = A_m m n_c. \quad (2)$$

The systems of simultaneous differential rate equations are solved using conventional Runge–Kutta algorithms with an adaptable time interval in the commercial program Mathematica. It is also noted that the use of 'stiff' differential equation solvers can lead to greatly improved computational speeds. The computer program consists of the main routine that contains the calls to the two main calculational and graphing subroutines. The calculational subroutine solves the set of differential equations using the appropriate initial values of the calling parameters ($n_c(0)$, $n_v(0)$, $n_s(0)$, $n_t(0)$, $m(0)$, $n_r(0)$, x, β). The graphing subroutine produces graphs of the electron and hole concentrations, $n_c(t)$, $n_v(t)$, $n_s(t)$, $n_t(t)$, $m(t)$ and $n_r(t)$, as a function of time, t, or temperature, T, and graphs of the TL glow curve, $I(T)$, as a function of the temperature. The numerical integration code for Mathematica was found to be very efficient, with typical computer times of a few minutes required for running the complete simulation.

Table 1 shows the parameters used in solving the rate equations, along with the original parameters of Chen and Leung[9,10].

A detailed comparison of the experimental superlinearity results for synthetic quartz with the results of the model of Chen and Leung has been given in detail elsewhere[14]. In that study, it was found necessary to make a few minor modifications to the parameters so that the model of Chen and Leung can also describe the experimentally observed superlinearity of pre-dosed and annealed quartz samples.

The following modifications to the parameters were introduced and are discussed in some detail in Ref. (14):

(a) The capacity of competitor states, N_s, was changed from 10^{12} to a value of 1.01×10^{13}.
(b) The capacity of reservoir states was changed from $N_r = 10^{13}$ to 10^{14} cm^{-3}.
(c) The probability, A_s, was changed from a value of 10^{-11} to 0.5×10^{-11} (cm^3 s^{-1}).

In addition to the above three modifications, the activation energy of the hole reservoir, R, was changed from $E_r = 1.4$ eV to a value of $E_r = 1.8$ eV in order to obtain an activation temperature of 500°C, which is typical of many natural varieties of quartz[1]. The rest of the parameters in the model of Chen and Leung[9,10] were left unchanged and are listed in Table 1.

Figure 1 shows in schematic form the steps simulated in the computer program. These steps include steps 1–7, taken during the additive dose technique, listed in the previous section.

The quartz sample is assumed initially to have zero occupancies of the electron and hole states, $n_s(0) = n_t(0) = m(0) = n_r(0) = 0$, at some point of time, $t = 0$, during its past. In the case of quartz, this time instant, $t = 0$, may correspond to the firing of the ceramic material during manufacturing, and it is assumed that the firing process erases the prior

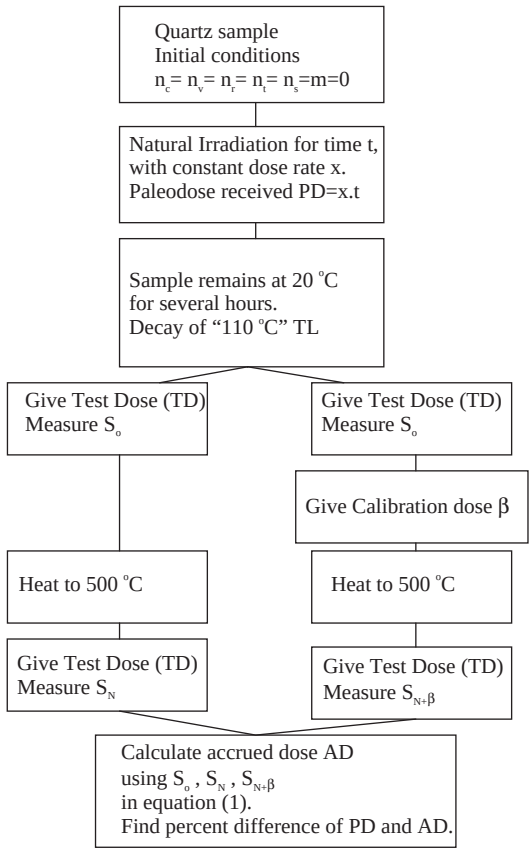

Figure 1. Schematic diagram of the various steps employed during the additive dose method in the pre-dose technique of thermoluminescence.

geological dose. During its subsequent 'lifetime', the material accumulates a natural PD. This 'natural irradiation' stage is simulated in the model by irradiating the quartz sample for a time period t in antiquity using a constant dose rate $x = 5 \times 10^8$ cm^{-3} s^{-1}. The PD received will be given by PD $= x \cdot t$ (in cm^{-3}).

The half-life of the 110°C TL peak in quartz at room temperature is only a few hours, resulting in this TL peak not being present in the glow curves of natural geological samples[15]. This fact is simulated in the present model by allowing the quartz sample to remain at room temperature for several hours after the natural irradiation step. This results in the decay of the concentration of trapped electrons in the 110°C trap T, so that $n_t(0) = 0$ for the next step in the simulation.

It is noted that the choice of the value of the ionisation rate, x, in kinetics models is to some extent arbitrary since in an experimental situation the ionization rate depends on the strength and proximity of the source, as discussed, e.g. in Ref. (15). For the present work, it is assumed that a pair production rate of $x = 5 \times 10^8$ cm^{-3} s^{-1} corresponds to an approximate dose rate of 0.01 Gy s^{-1}. This conversion factor from the dose units of cm^{-3} (used in this paper), to the more conventional dose units of gray, must be used as a rough approximation only, and it must be kept in mind that the exact conversion factor will depend on the actual experimental set-up.

It was found that on varying the natural dose rate by more than 10 orders of magnitude, from $x = 5 \times 10^2$ to 5×10^{12} cm^{-3} s^{-1} (while the laboratory dose rate was kept constant), the results of the model shown in Figure 4 remained unchanged. It can be concluded that the present model does not predict any dose rate effects, at least within these broad ranges of x-values.

In a typical experimental application of the pre-dose procedure, a TD value of 0.01 Gy is commonly used, as well as a calibration dose, β, typically equal to a few grays. In the present simulation, the small TD is arbitrarily taken to correspond to an irradiation time $t = 1$ s at a constant dose rate of $x = 5 \times 10^8$ cm^{-3} s^{-1}, resulting in a value of the TD of $x \cdot t = 5 \times 10^8$ cm^{-3}.

In some parts of the simulation, the value of the TD is varied within a few orders of magnitude, in order to study the effect of the TD on the accuracy of the pre-dose method. These data are shown in Figure 6.

The value of β in most parts of the simulation is taken to be approximately 100 times larger than the TD, with a value of $\beta = 5 \times 10^{10}$ cm^{-3}. In some parts of the simulation, the value of β is also varied within an order of magnitude in order to study the effect of the calibration dose on the accuracy of the pre-dose method. These data are shown in Figure 5.

The simulation calculates the percentage difference between the calculated AD from Equation 1 and the known value of the PD, over a wide range of PDs.

NUMERICAL RESULTS

Figures 2–4 show the results of the simulation using a fixed TD $= 5 \times 10^8$ cm^{-3} and a calibration dose, β, equal to 0.4 times the paleodose, $\beta = 0.4$(PD). The activation temperature is 600°C for all the data shown.

Figure 2 shows the dose response of the main traps (n_t), the competing traps (n_s), the luminescence centre (m) and the Zimmerman reservoir (n_r) over the PD range of PD $= 5 \times 10^8$–10^{11} cm^{-3}. This range of PD values corresponds to irradiation times $t = 1$–200 s.

Figure 3 shows the corresponding variations of the sensitivities S_o, S_N and $S_{N+\beta}$ with the PD, as calculated by the model. These three sensitivities are seen to vary linearly with the PD, indicating

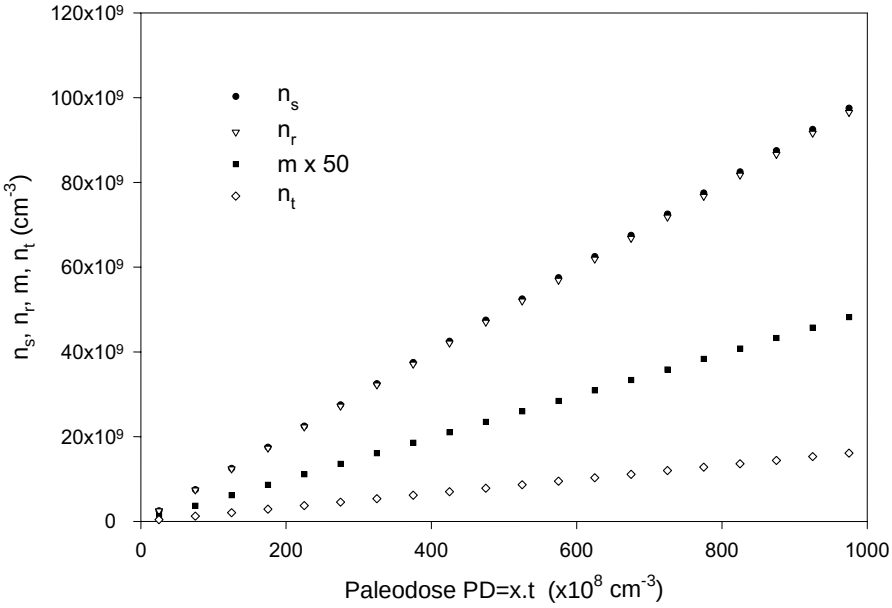

Figure 2. The dose response of the main traps (n_t), the competing traps (n_s), the luminescence centre (m) and the Zimmerman reservoir (n_r), over the PD range 5×10^8–10^{11} cm^{-3}. A fixed TD of 5×10^8 cm^{-3} and a calibration dose, β, of 0.4 PD are used.

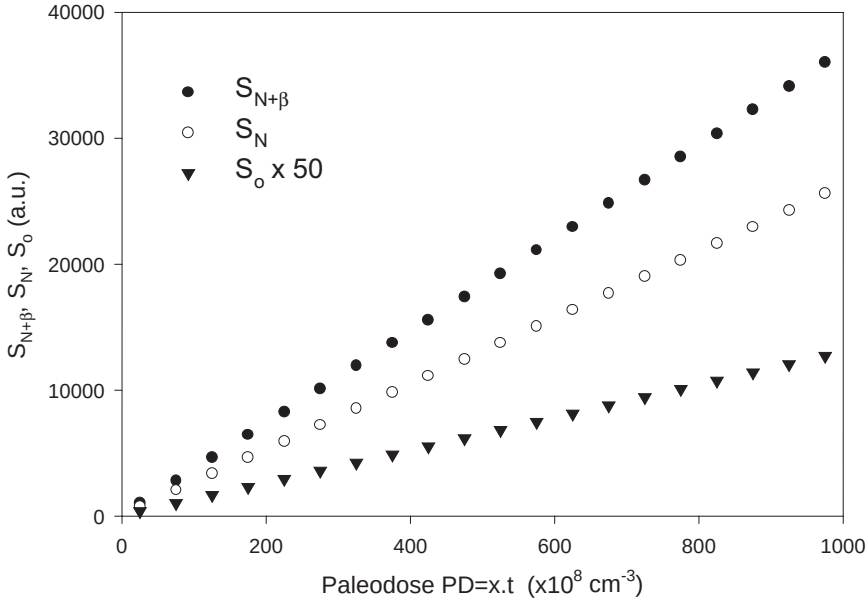

Figure 3. The linear variations of the sensitivities S_o, S_N and $S_{N+\beta}$ to the PD, as calculated by the model.

that in principle the pre-dose method should be applicable in this dose range. Figure 3 also shows that the value of S_o is about 100 times smaller than S_N, satisfying the requirement of 'low-S_o' values for applicability of the pre-dose technique[3].

The parameters in the model were chosen so that $S_o \ll S_N$, so that the pre-dose method will work. It is nevertheless possible to obtain an estimate of what happens to the accuracy of the method when the condition $S_o \ll S_N$ is not satisfied. By varying

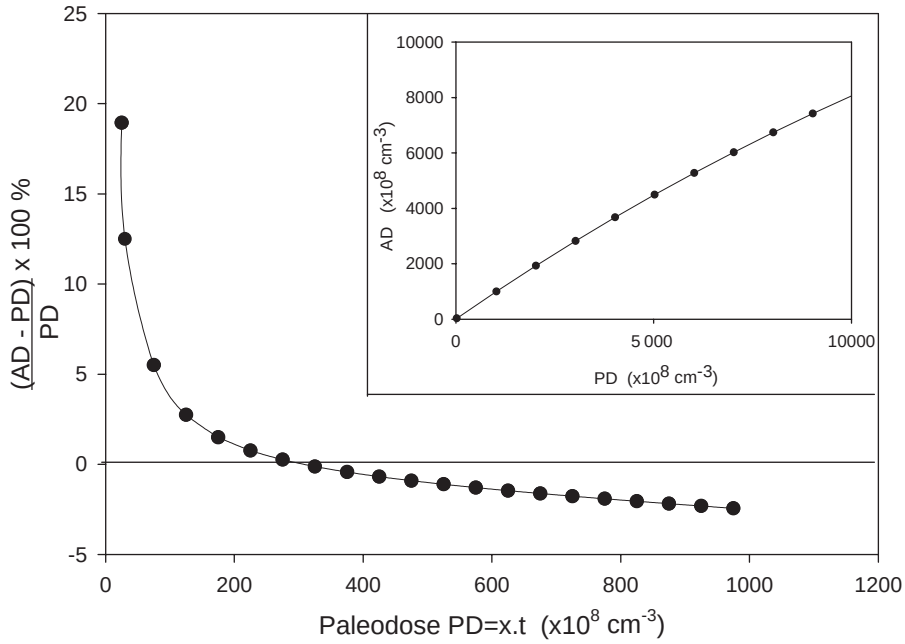

Figure 4. The variation of the accuracy of the calculated AD with the PD. The inset shows the same AD data extending over the non-linear region.

the retrapping probability of holes in the reservoir, A_r, from a value of $A_r = 10^{-10}$ cm^{-3} s^{-1} to a value of $A_r = 10^{-11}$ cm^{-3} s^{-1}, it is found that the ratio S_N/S_o is changed to a value of $S_N/S_o = 10$. This change in the ratio results in all the percentage accuracies shown in Figure 4 being smaller by 7%, thus reducing significantly the overall accuracy of the pre-dose method.

Figure 4 shows the percentage difference between the calculated AD and the PD. The data in Figure 4 show that the model reproduces accurately the PD received by the sample with an accuracy of ±2% or better. This accuracy is achieved over a range of PDs 75×10^8–10^{11} cm^{-3} (corresponding to irradiation times $t = 15$–200 s).

The accuracy of the method is seen to decrease for doses below PD $= 75 \times 10^8$ cm^{-3} and to approach a value of +20% at a very small values of the PD, 25×10^8 cm^{-3} (irradiation time of $t = 5$ s). This decrease in the accuracy of the method at low PDs can be expected on physical grounds as follows. At low PDs, the TD is of the same order of magnitude as the PD itself, and administration of the TD can alter the distribution of electrons and holes in the R, L, T and S centres. This leads to inaccuracies in the calculated AD.

For PDs larger than 10^{11} cm^{-3}, the sensitivities S_o, S_N and $S_{N+\beta}$ exhibit non-linear behaviour, which leads to larger inaccuracies in the calculated PD. This is shown in the inset of Figure 4, which shows the non-linear variation of AD with the PD for doses larger than $D = 10^{11}$ cm^{-3}.

By varying the parameter E_r in the range $E_r =$ 1.4–2.0 eV, it is found that the results of the simulation shown in Figure 4 remain essentially the same. Specifically, the percentage accuracy shown in Figure 4 is found to change by only 0.1% at the most, when the parameter E_r is changed within the above limits. Similarly, by varying the total concentration of the holes in the reservoir, N_r, within the range 10^{14}–10^{17} cm^{-3}, the percentage accuracy in Figure 4 changed by 0.1–1% at the most. Finally, the pair production rate, x, was varied in the range 10^2–10^9 cm^{-3} s^{-1}, and the results of Figure 4 show variations by 0.2% at the most.

Experimentally, it has been found that the results of the pre-dose technique may also depend on the calibration dose, β, given to the sample[13]. Figure 5 shows the variation of the accuracy of the simulation when the calibration dose is varied from 0.2 to 1.8 times the PD, with a fixed TD value of 5×10^8 cm^{-3}. The data in Figure 5 show that the accuracy of the simulation is improved at lower values of the calibration dose, β, but in all cases remain within the typical experimental accuracy of ±5%, over the PD range of Figure 5.

One might also expect on the basis of physical arguments that (a) the value of the TD would have some effect on the results of the pre-dose technique and (b) that the accuracy of the pre-dose method

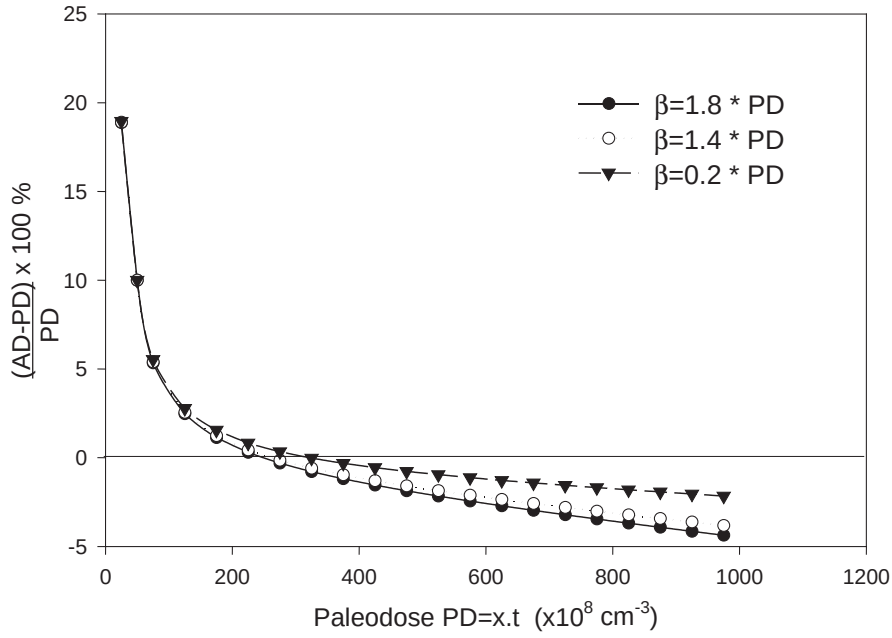

Figure 5. The variation of the accuracy of the calculated AD with the calibration dose, β. A fixed TD of 5×10^8 cm^{-3} is used.

might be improved by using as small a TD as possible. Figure 6 shows the results of varying the TD within the range 5×10^8–25×10^8 cm^{-3}. It is seen that the value of the test dose has a rather large effect on the accuracy, especially at low PDs. The results shown in Figure 6 imply that in an experimental situation the TD should be made as small as possible, within the experimental constraints imposed by the magnitude of the TL signal.

Figure 7 shows the concentrations of holes, $m(T)$ and $n_r(T)$, in the luminescence centre, L, and in the hole reservoir, R, correspondingly, as a function of the annealing temperature, T, during step 6 of the pre-dose procedure. The results of Figure 7 show that the model describes successfully the pre-dose activation process, which consists of the hole transfer from R to L during the heating of the sample to 600°C. As the temperature, T, increases, the concentration of holes, $m(T)$, in L is also increased, while the corresponding concentration of holes, $n_r(T)$ in the reservoir, R, is decreased by the same amount. The sum of the concentrations, $n_r(T) + m(T)$, remains constant, as required by charge conservation.

The results of Figure 7 also show that an activation temperature of 600°C is sufficiently high to transfer all holes from the reservoir, R, to the luminescence centre L. The exact value of the activation temperature is a function of the parameter values used in the present model—this dependence is the subject of a separate detailed study to be presented elsewhere[16].

In a separate part of the simulation, the thermal activation characteristic of the quartz sample was simulated and was found to be identical in shape to the graph $m(T)$ shown on Figure 7. Another important phenomenon described by the current model is the well-known radiation dose quenching of the sensitivity in quartz. This phenomenon, although interesting, is not used in the additive dose method in quartz, which is the main topic of this work, and will not be discussed here.

DISCUSSION AND CONCLUSIONS

The modified Zimmerman model presented in this paper simulates successfully the complete sequence of experimental steps taken during the AD version of the pre-dose technique. The solution of the kinetic equations elucidates the process of transfer of holes from the reservoir, R, to the luminescence centre, L, caused by the high temperature annealing. Furthermore, the model provides quantitative results on the effect of the TD and of the calibration dose, β, on the accuracy of the pre-dose technique.

The empirical assumptions of linear dependence of S_o, S_N and $S_{N+\beta}$ on the PD arise naturally within the model and are shown to lead to accurate

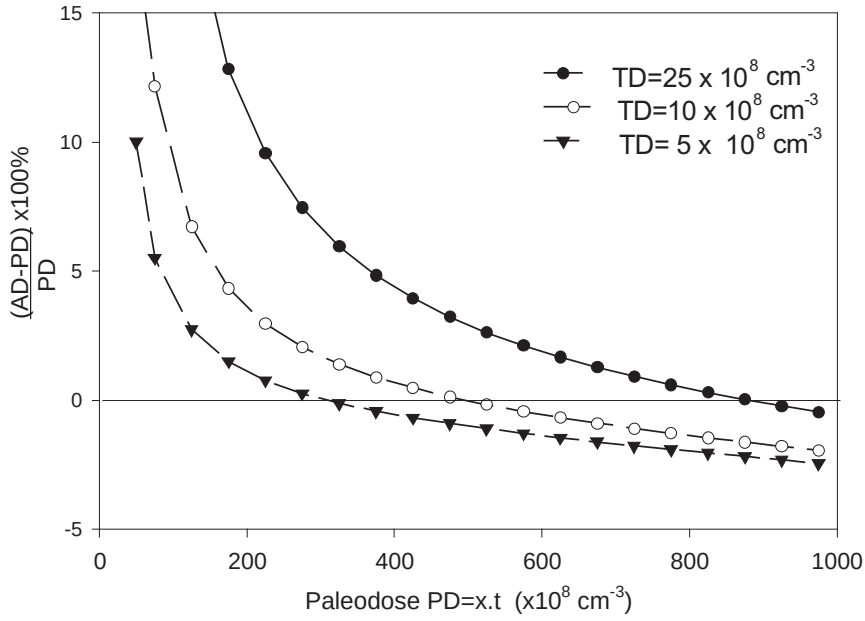

Figure 6. The effect of the TD on the accuracy of the simulation. A fixed calibration dose $\beta = 0.4$ PD is used.

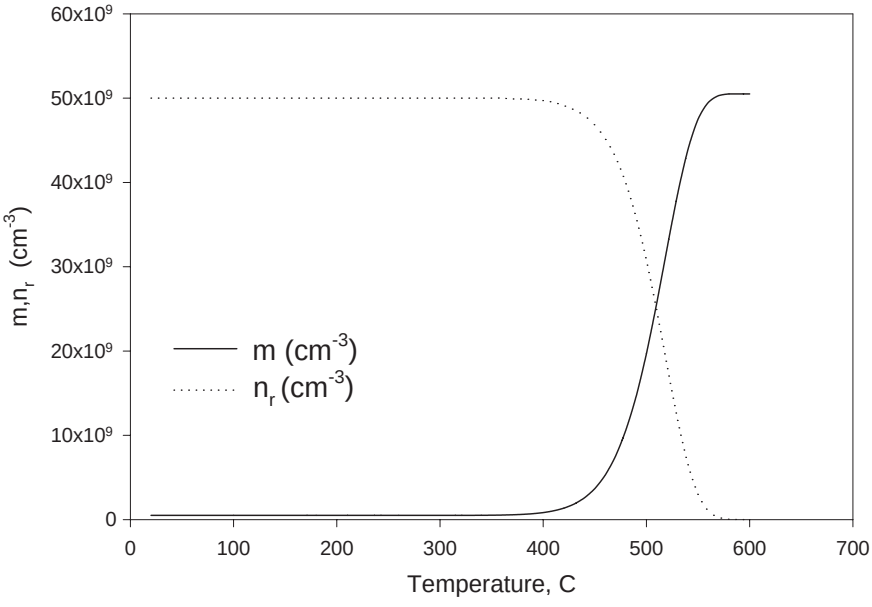

Figure 7. The variation of the concentration of holes ($n_r(T)$), $m(t)$, with the annealing temperature, showing the transfer of holes from R to L.

estimates of the value of PD over a wide range of PDs. The non-linear dependence of these sensitivities on the PD is shown to lead to inaccuracies in the calculated AD.

Preliminary results show that the model presented in this paper can also be used to simulate the multiple activation procedure of the pre-dose technique. The multiple activation procedure is experimentally

slightly more complicated than the AD technique simulated here due to (a) the need to activate thermally the sample more than once by heating to 500°C and (b) the presence of the well-known radiation quenching effect in quartz. This work is in progress currently, and the results will be presented elsewhere.

It is noted that a more general but similar kinetic model for quartz has been published by Bailey[15]. This model contains four hole trapping centres and five electronic trapping centres described by a total of 44 kinetic parameters, while the current model contains a total of just four energy states described by 13 kinetic parameters. Despite its simplicity, the current four-level model of Chen and Leung[10] has been shown to be very effective in describing several of the important characteristics of the pre-dose effect, as listed previously in this paper. The conclusions drawn from the simple quartz model presented here can be used to make improvements to the values of the parameters in the more general model of Bailey[15]. This work is in progress currently.

It is also noted that at least two different approaches that are based on specific impurities in quartz crystals have been proposed for explaining the pre-dose effect. Yang and McKeever[17] proposed that the pre-dose effect might be due to the movement of hydrogen ions between defects during the irradiation and annealing steps of the pre-dose technique. A second physical model based on quartz impurities was suggested recently by Itoh *et al.*[18]. Their model is based on known impurities and defect processes in quartz as well as on the introduction of an additional ionic process. The model of Itoh *et al.*[18] provides important evidence for a link between the pre-dose effect and known impurities and defect centres in quartz. Clearly, additional theoretical work is necessary in order to incorporate the results of these two alternative approaches in the current kinetic model.

In summary, the results of the model can be compared with the actual experimental data on quartz as follows:

(a) The model predicts that the additive dose technique is accurate with an accuracy of at least ±5%, within approximately two orders of magnitudes of the PD. This is in agreement with the experimental results in Ref. (4–7).
(b) The model predicts the correct shape for the experimentally measured thermal activation characteristic in quartz (TAC), which is shown as the curve $m(T)$ in Figure 7. This is in agreement with the most common form of experimentally measured TAC for quartz in the literature[1].
(c) The model predicts that the value of the laboratory dose, β, has a small but important effect on the accuracy of the additive dose method, as shown in Figure 5. This is in qualitative agreement with the experimental results in Ref. (13).

ACKNOWLEDGEMENTS

The authors wish to thank Dr Reuven Chen for a preliminary reading of this manuscript and for several useful suggestions. The financial support of Dr S. Case, Dean of Faculty at McDaniel College, and of the Faculty Development Committee at McDaniel College are gratefully acknowledged.

REFERENCES

1. Bailiff, I. K. *The pre-dose technique.* Radiat. Meas. **23**, 471–479 (1994).
2. Haskell, E. H. *Retrospective accident dosimetry using environmental materials*. Radiat. Prot. Dosim. **47**(1/4), 297–303 (1993).
3. Aitken, M. J. *Thermoluminescence Dating* (London: Academic Press) (1985) ISBN 012-0463806.
4. Bailiff, I. K. and Haskell, E. H. *The use of the pre-dose technique for environmental dosimetry*. Radiat. Prot. Dosim. **6**, 245–248 (1984).
5. Stoneham, D. *The use of porcelain as a low-dose background dosimeter*. Nucl. Tracks **10**, 509–512 (1985).
6. Haskell, E. H., Kaipa, P. L. and Wrenn, M. E. *Pre-dose TL charactristics of quartz inclusions removed from bricks exposed to fallout radiation from atmospheric testing at the Nevada test site*. Nucl. Tracks Radiat. Meas. **14**, 113–120 (1988).
7. Haskell, E. H., Bailiff, I. K., Kenner, G. H., Kaipa, P. L. and Wrenn, M. E. *Thermoluminescence measurements of gamma-ray doses attributable to fallout from the Nevada Test Site using building bricks as natural dosimeters*. Health Phys. **66**, 380–391 (1994).
8. Hutt, G., Brodksi, L., Bailiff, I. K., Goksu, Y., Haskell, E., Jungner, H. and Stoneham, D. *Accident dosimetry using environmental material collected from regions downwind of Chernobyl: a preliminary evaluation*. Radiat. Prot. Dosim. **47**, 307–311 (1993).
9. Chen, R. and Leung, P. L. *Processes of sensitization of thermoluminescence in insulators*. J. Phys. D: Appl. Phys. **31**, 2628–2635 (1998).
10. Chen, R. and Leung, P. L. *Modeling the pre-dose effect in thermoluminescence*. Radiat. Prot. Dosim. **84**, 43–46 (1999).
11. Zimmerman, J. *The radiation induced increase of the 100°C TL sensitivity of fired quartz*. J. Phys. C: Solid State Phys. **4**, 3265–3276 (1971).
12. Zimmerman, J. 1971. *The radiation induced increase of the thermoluminescence sensitivity of the dosimetry phosphor LiF (TLD-100)*. J. Phys. C: Solid State Phys. **4**, 3277–3291 (1971).
13. Chen, R. *Saturation of sensitization of the 100°C TL peak in quartz and its potential application in*

the pre-dose technique. Eur. PACT J. **3**, 325–335 (1979).
14. Pagonis, V., Kitis, G. and Chen, R. *Applicability of the Zimmerman pre-dose model in the thermoluminescence of pre-dosed and annealed synthetic quartz samples*. Radiat. Meas. **37**, 267–274 (2003).
15. Bailey, R. M. *Towards a general kinetic model for optically and thermally stimulated luminescence in quartz*. Radiat. Meas. **33**, 17–45 (2001).
16. Chen, R. and Pagonis, V. *Modeling thermal activation characteristics of the sensitization of thermoluminescence in quartz*. J. Phys. D: Appl. Phys. **37**, 159–164 (2004).
17. Yang, X. H. and McKeever, S. W. S. *Characterization of the pre-dose effect using ESR and TL*. Nucl. Tracks Radiat. Meas. **14**, 75–79 (1988).
18. Itoh, N., Stoneham, D. and Stoneham, A. M. *The pre-dose effect in thermoluminescent dosimetry*. J. Phys. Cond. Matter **13**, 2201–2209 (2001).